Article

Journal of Nanoscience and Nanotechnology
Vol. 15, 3757–3763, 2015
www.aspbs.com/jnn

Synthesis of $LiNbO_3$ Nanoparticles by Citrate Gel Method

C. Debnath, S. Kar, S. Verma, and K. S. Bartwal*

Laser Materials Development and Devices Division Raja Ramanna Centre for Advanced Technology, Indore 452013, India

We present investigations on the preparation of nearly stoichiometric lithium niobate ($LiNbO_3$) nanoparticles using citrate gel method. Citric acid is used as a chelating agent and ethylene glycol is added for polyestarification between the chelates. In addition to the main lithium niobate phase, the secondary phase of lithium niobate, $LiNb_3O_8$, and an unreacted phase of Nb_2O_5 were also observed in the resultant product. The appearance of unwanted phases is a serious problem in citrate gel method. We have observed that the synthesis parameters such as molar ratio of citric acid to metal ions (R_1), pH, molar ratio of ethylene glycol to citric acid (R_2) and calcination temperature strongly influence the presence of the unwanted phases and these parameters are optimized to remove these phases. Evolution of the phase was investigated by powder XRD whereas TG/DTA was done to find out the crystallization temperature. It was observed that nearly stoichiometric and pure $LiNbO_3$ nanoparticles can be obtained with the optimized parameters, $R_1 = 3$, pH $= 8$, $R_2 \geq 2$ and calcination temperature $= 700$ °C. The stoichiometry of the synthesized $LiNbO_3$ nanoparticles was investigated using Raman spectroscopy.

Keywords: Lithium Niobate, Sol–Gel Preparation, X-Ray Techniques, Electron Microscopy, Raman Spectroscopy.

1. INTRODUCTION

Nanomaterials research is currently an area of intense scientific interest due to potential applications in biomedical, optical and electronic fields. The basic understanding of the nanoparticles and their properties have been extensively compiled in the 25 volumes of the "Encyclopedia of Nanoscience and Nanotechnology" edited by Nalwa.[1] Due to quantum-confinement effects nanomaterial's electronic and optical properties are drastically different from its bulk counterpart. Lithium niobate, $LiNbO_3$ (LN) is one of the important optical and electronic materials having photorefractive, acousto-optic, nonlinear optic, electro-optic, ferroelectric, piezoelectric, pyroelectric properties, which make it a promising candidate for many applications such as light modulation, optical wave guides, second harmonic generation devices, optical parametric oscillation devices, holographic memory devices, surface acoustic wave devices etc.[2–5] However, its various properties strongly depend on stoichiometry.[6,7] Many routes have been developed for synthesis of LN nanoparticles resulting in different size, shape and crystalline quality. Traditionally, LN is prepared by solid state reaction at high temperature above 1100 °C which leads to inhomogeneity in composition deviating from stoichiometry because of serious evaporation of Li_2O component resulting in the niobium ions to change the valence state.[7,8] In recent years, LN nanocrystalline powders were synthesized using wet chemical methods such as co-precipitation,[9] sol–gel,[10] hydrothermal,[11] colloid emulsion,[12] molten salt,[13] from water soluble maleic acid complex,[14] low temperature solution phase reduction of niobium (V) chloride using lithium hydride[15] etc. These wet chemical methods have many unique advantages due to lower processing temperature, easier composition control and better homogeneity of prepared LN nanocrystalline powders. Sol–gel using alkoxides, hydrothermal and colloid emulsion routes are time consuming and involve highly unstable metal alkoxides which are highly inflammable, relatively high cost, and high sensitivity to moisture and hence difficult to maintain reaction conditions. Pechini method[15] solves the problem of niobium alkoxide by using some α-carboxylic acid (e.g., citric acid) to coordinate with the niobium ions. The Pechini method is a wet chemical technique offering many advantages such as homogeneous mixing at molecular level, better stoichiometric control, low processing temperature and the production of desired powder.

*Author to whom correspondence should be addressed.

 1533-4880/2015/15/3757/007 doi:10.1166/jnn.2015.9769

Thus Pechini method is a convenient method for synthesis of oxide nanoparticles. Pechini method using citric acid as a chelating agent is also termed as citrate gel method. In recent years a large number of oxide nanoparticles have been synthesized, which are promising for photonics applications.[16–22]

In the present work we adopted the citrate gel method for synthesizing LN powder using niobium oxide, lithium nitrate, citric acid (CA) and ethylene glycol (EG) as raw materials. Along with the main $LiNbO_3$ phase the secondary phase of lithium niobate, $LiNb_3O_8$, and an unreacted phase of Nb_2O_5 were also observed in the obtained powder precursor. Appearance of these two phases is undesirable and required proper optimization of various synthesis parameters to get rid of these phase. The presence of the unwanted phase was found to depend strongly on the molar ratio of CA to metal ions (R_1), molar ratio of EG to CA (R_2), pH of the reaction mixture and calcination temperature. We have performed parametric investigations of the above synthesis parameters to remove these unwanted phases. We have used the X-ray powder diffraction (XRD) technique to characterize and confirm the phase, stoichiometry and crystallinity after each synthesis experiment. TG/DTA was done to find the crystallization temperature. The size of the particles was obtained by powder XRD data, transmission electron microscopy (TEM) and dynamic light scattering (DLS) experiments. The stoichiometry of the particles was characterized by Raman spectroscopy.

2. EXPERIMENTAL PROCEDURE

Niobium (V) oxide (Alfa Aesar, 99.9%), lithium nitrate (Merck, 99.995%), hydrofluoric acid (Merck, 48% GR), citric acid anhydrous (Fisher Scientific, SQ) and ethylene glycol anhydrous (Sigma Aldrich, 99.8%) were used as the starting materials. A stoichiometric amount of $LiNO_3$ was dissolved in de-ionized water to form lithium hydroxide (LiOH) and Nb_2O_5 was dissolved in HF after heating in a water bath at 38 °C for at least 20 h to form niobium fluoride (NbF_5). For the preparation of Li–Nb–CA precursor solution, the clear solutions of LiOH and NbF_5 were mixed in the aqueous solution of CA separately in two beakers with continuous stirring. Then the solution of lithium citrate was mixed with the solution of niobium citrate drop by drop with continuous stirring. At this stage the molar ratio of the CA to metal ions (defined by R_1) was varied from 1 to 4. The pH was varied (1.2, 4.0, 6.1, 8, and 9.7) by adding ammonia solution and nitric acid. Then EG was added to promote mixed citrate polymerization by polyesterification reaction and the molar ratio of EG to CA (defined by R_2) was varied (0 to 5 with step of 0.5). The obtained Li–Nb–CA precursor solution was heated at 80 °C to produce a gelatinous precursor after evaporation of water. Subsequently, the gel was calcined in air atmosphere by heating successively at various temperatures (550, 600, 650, 700, 750 and 800 °C for 5 h each) which are well above the crystallization temperature as determined from TG/DTA experiment (Setaram TG-DTA 92B). Finally the powder samples were formed after calcination.

The powder XRD patterns were recorded for all the samples with step size of 0.01° and scanning speed of 5 °/min using X-ray diffractometer (Rigaku, Geigerflex). The particle size was determined by TEM (Philips, Tecnai G^2-20 (FEI)), DLS (Zetasizer Nano ZS90; ZEN-3690) and XRD peak width. Before performing DLS the LN powders were suspended in de-ionized water homogeneously by several stirring followed by ultrasonication. The particles were also characterized by micro-Raman spectroscopy (Labram-HR800) in backscattering geometry using an Ar^+ excitation source ($\lambda = 488$ nm) and concentration of Li in mol%, $c_{Li} = [Li]/([Li]+[Nb])$, in LN crystal was obtained.

3. RESULTS AND DISCUSSION

The citrate gel technique was used to prepare the single phase LN nanoparticles. The outcome of this method depends on the formation of complexes of alkali metals, transition metals, or even non-metals with mono-, bi-, and tridentate organic chelating agent like CA. The polyalcohol, EG is added to establish linkages between the chelates by polyestarification reaction, resulting in gelation of the reaction mixture. Unlike traditional sol–gel processes, where the metal itself becomes an integral part of the gel network, in this method the gel network is formed by the esterification of the chelating agent and polyalcohol. The metal ions are essentially trapped in the organic matrix, to which they are weakly bound. Hence it is also known as modified sol–gel method. The formation of the complexes of alkali metals (e.g., Li), transition metals (e.g., Nb) with CA relies on the amount of CA (i.e., on the value of R_1). For higher amount of CA more

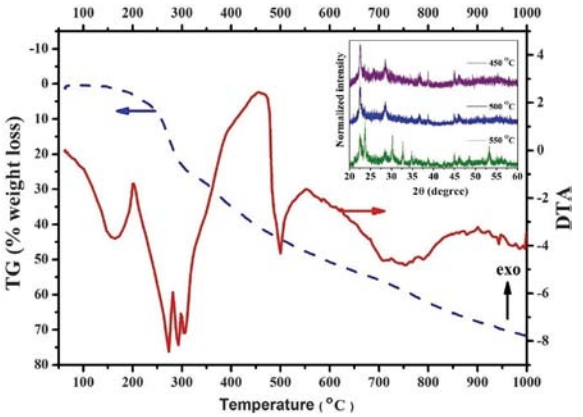

Figure 1. Simultaneous TG/DTA investigations of preheated Li–Nb–citrate gel in static argon atmosphere with heating rate 10 °C/min; The inset graph shows the XRD peaks at different calcination temperatures.

carboxylic groups (COO^-) can be available to chelate the metallic ions in the solution.

A black–brown powder was obtained by heating the precursor gel at 200 °C for 1 h. The TG/DTA investigations in static Ar-atmosphere were carried out on this preheated powder with a heating rate 10 °C/min as shown in Figure 1. In the TG graph significant weight loss doesn't occur up to 200 °C. But in this range there is a strong endothermic peak in the DTA graph arising due to melting of the Li–Nb–CA precursor and removal of remaining water from precursor. Above 200 °C there is a rapid weight loss in the TG graph due to decomposition of the precursor and in the DTA graph there is a strong endothermic peak at about 300 °C. It has been observed that the descending portion of the decomposition endotherm covers the temperature interval of the main weight loss step and this endothermic peak occurs in a multi-step process.[23] The associated exothermic peaks suggest a self-combustion-like process in which nitrate ions act as an oxidizing agent and CA as fuel. After this endothermic peak three broad exothermic peaks arises due to crystal formation at the temperatures about 450, 550 and 890 °C respectively. The first exothermic peak arises due to oxidization of the niobium ions in the form of Nb_2O_5 confirmed by XRD. The second exothermic peak arises due to crystal formation of lithium–niobium–oxygen compound in the form of $LiNb_3O_8$ and $LiNbO_3$, also confirmed by XRD analysis. Above 550 °C, $LiNb_3O_8$ decomposes to convert into $LiNbO_3$ and at the temperature about 750 °C, $LiNb_3O_8$ phase becomes negligible. After this the exothermic peak arises due to growth of $LiNbO_3$ particles. There is still some weight loss in the TG curve even at the higher temperature range as the evaporation rate of the organic compounds in oxide form is much weaker in Ar-atmosphere.

Therefore in citrate gel method Nb_2O_5 and $LiNb_3O_8$ arise as unwanted phase in the resultant product. We have optimised the experimental parameters to remove these unwanted phases. The powders prepared from various molar ratio of CA to metal ions, R_1 (1, 2, 3, and 4) with stoichiometric pH value (~2.8–3.0), molar ratio of EG to CA, $R_2 = 1$ and calcination temperature 650 °C were examined by XRD, as shown in Figure 2(a). Here all the XRD patterns are normalized and put in the same scale to make a comparative study. It was found that the precursor contains a higher amount of $LiNbO_3$ phase and little amount of un-reacted Nb_2O_5 and $LiNb_3O_8$ phases which are minimum at $R_1 = 3$. Miller indices corresponding to the dotted lines are of pure hexagonal phase of stoichiometric $LiNbO_3$ structure (JCPDS no. 20-0631). At lower value of R_1, due to lack of sufficient COO^- groups the chelation of the metal ions is not completed. At sufficiently higher value of R_1 the concentration of the metal ions in the complex host matrix becomes very less and hence some of them are unable to react each other resulting in segregation with heating process. Therefore, here the optimum value of R_1 is 3. With stoichiometric *pH* value, $R_2 = 1$ and $R_1 = 3$ the effect of calcination temperature

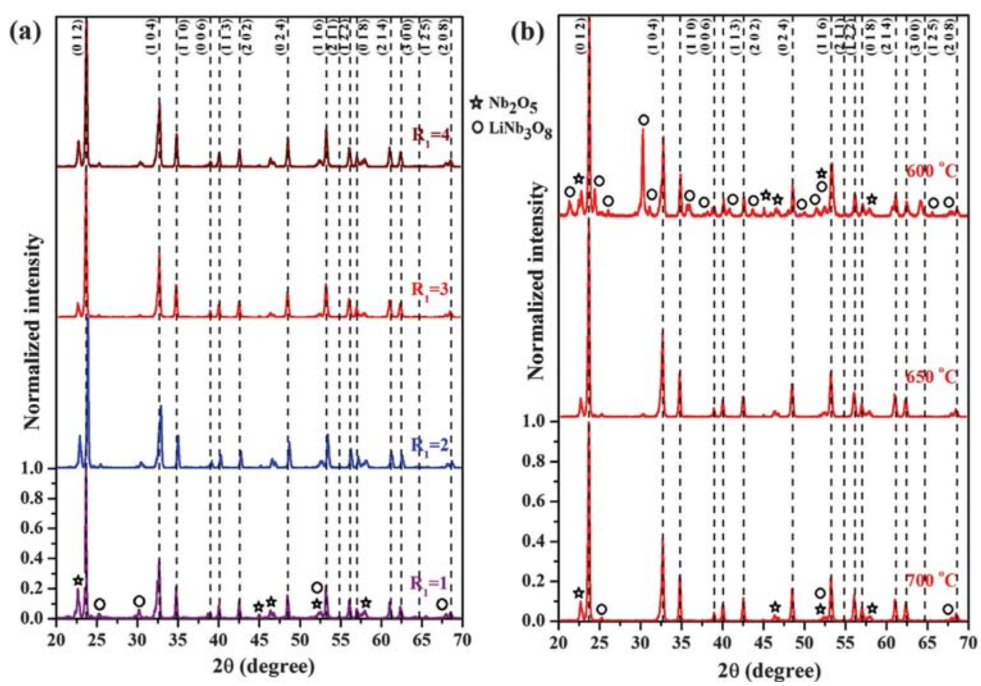

Figure 2. Normalized XRD spectra of the samples for (a) various R_1, $R_2 = 1$, stoichiometric pH value and calcination temperature 650 °C; (b) $R_1 = 3$, $R_2 = 1$, stoichiometric pH value and various calcination temperature.

on the unwanted phases is shown in Figure 2(b) and it was observed that at higher temperature (650 °C or above) the $LiNb_3O_8$ phase is greatly reduced. Generally lithium forms ionic coordination with CA whereas niobium may form mono-, bi- or tridentate chelating complex depending upon the availability of COO^- groups surrounding it. The lower decomposition temperature of ionic ligand makes the chelating of metal ions (e.g., Li^+ ions) with COO^- group to collapse easily than bi- or tri-dentate ligands. Therefore, in lower heating process the Li^+ ion coordinated with COO^- would be much easier to segregate and find relatively lesser amount of Nb ions to react and may form another compounds (not found in XRD patterns). Hence at moderate temperature (e.g., 600 °C or below) relatively smaller amounts of Li ions are available to react with Nb-ions resulting in lithium deficient phase $LiNb_3O_8$ (JCPDS no. 75-2154) as a dominating phase. As the calcination temperature increases (650 °C, 700 °C, etc.), a solid state reaction between $LiNb_3O_8$ and Li-compounds occurs to form $LiNbO_3$ phase resulting in the reduction of $LiNb_3O_8$ phase. In Figure 2(b), it is also observed that there is an insufficient change in Nb_2O_5 phase with calcination temperature due to incomplete chelation as explained above. The order of chelation increases with pH because at higher pH conditions, more CA is ionized by ionizing the COOH group and hence more COO^- groups can be available to chelate the metallic ions in the precursor solution. Hence keeping the value of R_1 fixed to 3, pH of the precursor solution was changed and effect of pH on the XRD phases of the precursor powder calcined at 650 °C is shown in Figure 3(a). It is found that at lower pH, the un-reacted Nb_2O_5 phase becomes dominating due to incomplete chelation for the lack of COO^- groups. With increasing pH, Nb_2O_5 phase reduces due to increasing degree of chelation as at higher value of pH more available COO^- groups allow the molecules to behave as bi-, tri, or tetra-dentate ligands increasing binding ability of CA. We have observed that the Nb_2O_5 phase completely disappear when the pH value was increased to 8. Therefore, at pH = 8 all the Nb-ions are able to complete the chelate formation with CA. It is also observed that the $LiNb_3O_8$ phase is dominating with pH due to higher decomposition temperature of bi- or tri- or tetradentate ligands associated with Nb atoms as explained above. Therefore, to react $LiNb_3O_8$ with segregated Li-compounds higher temperatures are required. In Figure 3(b) we have shown the effect of calcination temperature on the phase of the precursor powders synthesized with $R_1 = 3$, $R_2 = 1$ and pH = 8. Here it is observed that at calcination temperature of 650 °C the $LiNb_3O_8$ phase remains in large extent and decreases adequately when the calcination temperature is increased to 700 °C and no further significant reduction occurs with higher calcination temperature as in this temperature range Li-cation diffuses easily; even it can evaporate from the raw materials.[12] Therefore, to remove the $LiNb_3O_8$ phase the segregation of Li-cation should be restricted and it

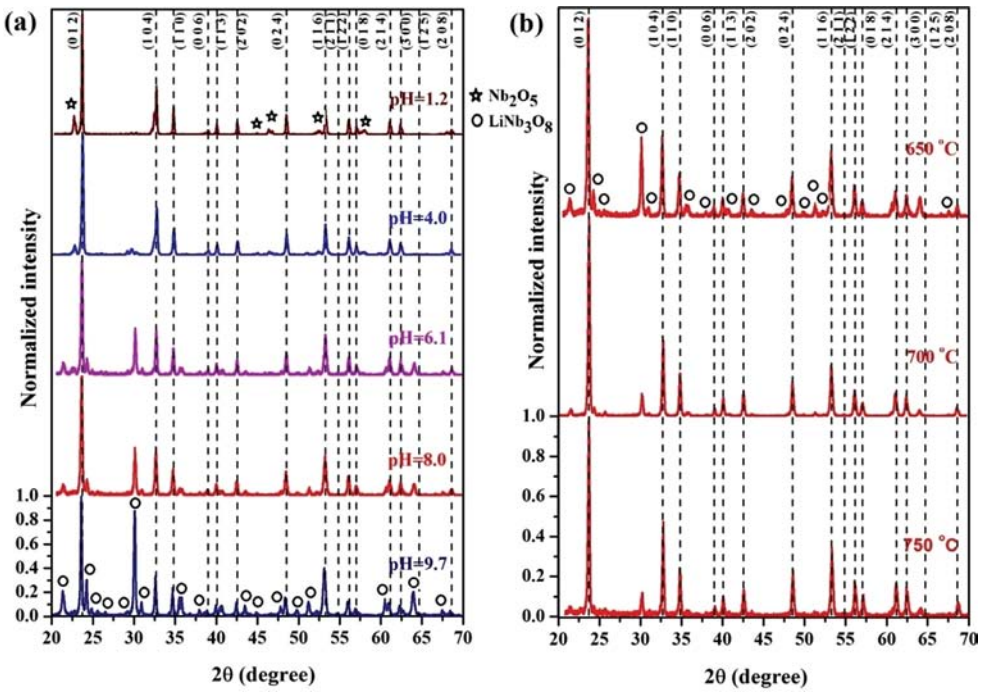

Figure 3. Normalized XRD spectra of the samples for (a) $R_1 = 3$, $R_2 = 1$, various *pH* value and calcination temperature 650 °C; (b) $R_1 = 3$, $R_2 = 1$, pH = 8 and various calcination temperature.

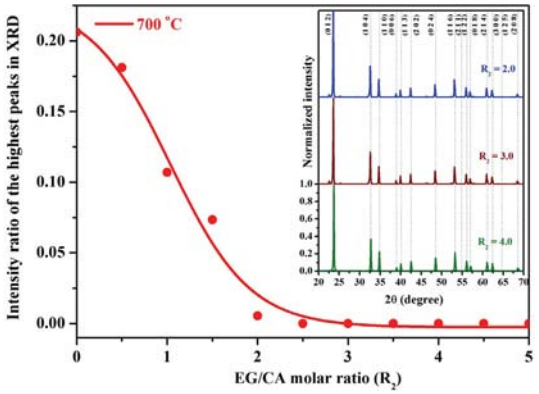

Figure 4. Intensity ratio of the highest XRD peaks of $LiNb_3O_8$ phase to the desired $LiNbO_3$ phase with $R_1 = 3$, pH = 8 and calcination temperature 700 °C and various EG to CA molar ratio R_2. The inset XRD patterns are for EG/CA molar ratio of 2, 3 and 4 respectively.

is possible by introducing more complex network to the gel with the help of the polymerising agent EG which can make polyestarification reaction between the citrate chelates. Keeping $R_1 = 3$, pH = 8, the effect of EG to CA molar ratio (R_2) to the $LiNb_3O_8$ phase for calcination temperature of 700 °C is shown in Figure 4. Here we have shown the variation of the relative intensity of the highest XRD peak of $LiNb_3O_8$ phase with respect to the highest XRD peak of $LiNbO_3$ phase. It has been observed that for $R_2 \geq 2$ the $LiNb_3O_8$ phase vanishes completely.

The distribution of particle sizes for the particles prepared with $R_1 = 3$, $R_2 = 2$, pH = 8 and calcination temperature 700 °C were obtained by TEM and DLS as shown in Figure 5, and it was found that the size of the particles is 91.5 nm with a variation of width 43.7 nm. The second peak at 238.6 nm in DLS spectrum arises due to agglomerated particles. The average crystalline volume can also be calculated by Scherrer's formula ($t = K\lambda/\beta\cos\theta_\beta$) from XRD peak at θ_β of width β assuming $K = 0.9$ (spherical particle) where λ is the wavelength of X-ray radiation. We have found that $t \cong 87$ nm.

LN belongs to the 3 m point group and R3c space group symmetry at room temperature the primitive cell of which contains two formula units (10 atoms) giving 30 degrees of vibrational freedom. At zero wave vector approximation, vibration may be characterized by group theory as $5A_1$, $5A_2$ and doubly degenerate $10E$ phonon branches of which one A_1 and one E are the three acoustic branches and five A_2 fundamentals are Raman and infrared inactive. Therefore, the total Raman effective modes are found to be $(4A_1 + 9E)$. However, long range electrostatic field in the ionic crystal lifts the degeneracy between longitudinal (LO) and transverse (TO) optical phonons and hence doubling the 13 observed phonons. Thus ideally, total 26 phonon modes are possible to detect by Raman spectroscopy in LN.[24] However, the total degeneracy is not achieved due to small variation in stoichiometry. The Raman spectrum for the particles prepared with $R_1 = 3$, $R_2 = 2$, pH = 8 and calcination temperature 700 °C is shown in Figure 6(a). In the present Raman investigation we have observed 17 peaks for the corresponding A_1(TO), A_1(LO), E(TO) and E(LO) modes. The observed Raman modes listed in the Table I are very close to the previously reported values.[25] Here the doublet modes are at 273 cm^{-1} (A_1(TO)/A_1(LO)), 332 cm^{-1} (A_1(TO)/A_1(LO)) and 430 cm^{-1} (A_1(LO)/E(LO)). The exact composition $c_{Li} = [Li]/([Li]+[Nb])$ of the LN crystal can be found from the line-width of some Raman lines.[26] They have chosen two Raman peaks one at about lower frequency, 153 cm^{-1} and the other at about higher frequency, 876 cm^{-1}. It has been reported[26,27] that the line width of the phonon mode at about 153 cm^{-1} is accompanied by an additional weak band at about 175 cm^{-1} which arises in the stoichiometric composition of LN crystal as shown (hump like) in Figure 6. The concentration of Li in LN can be obtained by using the formulae:

$$c_{Li}[\text{mol}\%] = 53.29 - 0.1837\Gamma_{875}[\text{cm}^{-1}];$$

for the Raman peak at 875 cm^{-1} and

$$c_{Li}[\text{mol}\%] = 53.03 - 0.4739\Gamma_{152}[\text{cm}^{-1}];$$

for the Raman peak at 152 cm^{-1}

Here Γ represents full width at half maxima of the Raman peak. By decoupling Raman peaks with Lorentzian

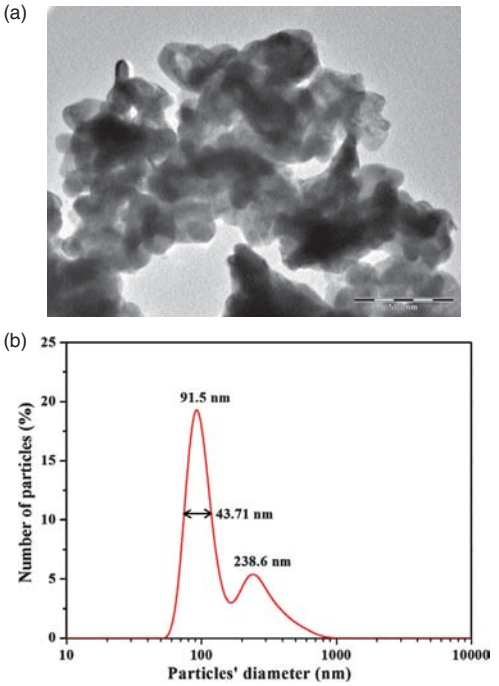

Figure 5. (a) TEM image; (b) The DLS spectrum for particle size distribution of the samples prepared with $R_1 = 3$, $R_2 = 2$, pH = 8 and calcination temperature 700 °C.

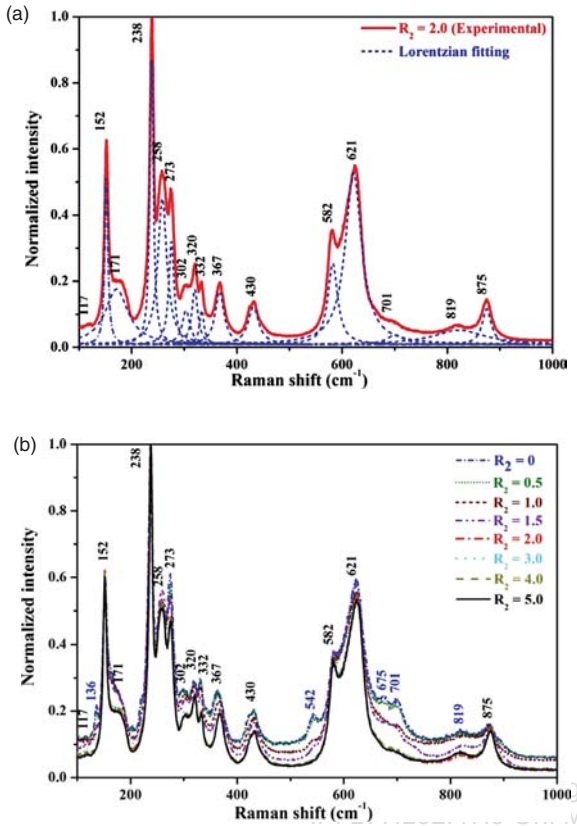

Figure 6. (a) Normalized Raman spectrum of $LiNbO_3$ powder sample prepared with $R_1 = 3$, $R_2 = 2$, pH = 8 and calcination temperature 700 °C. (b) Normalized Raman spectra of $LiNbO_3$ powder samples prepared with $R_1 = 3$, pH = 8, various R_2 (0, 0.5, 1.0, 1.5, 2.0, 3.0, 4.0 and 5.0) and calcination temperature 700 °C.

fitting and from the peak widths Γ_{875} and Γ_{152} we have calculated c_{Li}[mol%] of value 49.50 and 49.61 respectively by using above empirical formulae. Thus on average $c_{Li} =$ 49.56 mol%. We have also observed that for $R_2 > 2$ the concentration of Li, $c_{Li} \cong 49.6$ mol%. Therefore our prepared LN nanoparticles are nearly stoichiometric.

In Figure 6(b) we have shown the Raman spectra for different R_2 (with $R_1 = 3$, pH = 8, calcination temperature = 700 °C). All the spectra are normalized with their maximum intensity and plotted in the same scale for comparison. For $R_2 = 0$, the Raman peaks at 136, 542,675 and 701 cm^{-1} arise due to the presence of $LiNb_3O_8$ phase.[28] With increase of R_2 these peaks are tending to disappear for reduction of $LiNb_3O_8$ phase as seen in Figure 4 and become negligible for $R_2 \geq 2$. We have also observed that for $R_2 < 2$ the Li concentration in LN is in the range of 48–49 mol%, i.e., congruent composition.

Table I. Observed bands (cm^{-1}) of several fundamental optical modes of Raman spectrum in $LiNbO_3$ at room temperature and a comparison with the previous Raman data.[25]

Observed band (cm^{-1})				Reference [25]			
A_1 (TO)	A_1 (LO)	E (TO)	E (LO)	A_1 (TO)	A_1 (LO)	E (TO)	E (LO)
258	273	152	117	253	273	152	117
273	332	238	171	275	331	238	198
332	430	320	302	334	428	322	298
	875	367	430		874	368	428
		582	621			582	621

4. CONCLUSIONS

The amount of CA, EG, pH of the precursor solution and the calcination temperature play an important role to synthesize single phase $LiNbO_3$ powder samples by citrate gel method. The unwanted of $LiNb_3O_8$ and Nb_2O_5 phase can be removed by optimizing the synthesis parameters which are molar ratio of CA to metal ions (R_1), molar ratio of EG to CA (R_2), pH of the reaction mixture and calcination temperature. We have found that the chelation of Nb ions with CA is completed when pH of the precursor solution be 8 with $R_1 = 3$ and unreacted Nb_2O_5 phase in the resultant product is disappeared. The Li deficient phase of $LiNb_3O_8$ can be removed by restricting the Li segregation by introducing sufficient ($R_2 \geq 2$) polymerising agent EG for polyestarification between the citrate chelates. Nearly stoichiometric (~49.6 mol% Li concentration) $LiNbO_3$ nanoparticles (below 100 nm diameter) can be obtained by citrate gel method with $R_1 = 3$, $R_2 \geq 2$, pH = 8 and calcination temperature of 700 °C.

References and Notes

1. H. S. Nalwa (Ed.), Encyclopedia of Nanoscience and Nanotechnology, American Scientific Publishers, LA **(2004/2011)**, Vols. 1–25.
2. R. S. Weis and T. K. Gaylord, *Appl. Phys. A* 37, 191 **(1985)**.
3. F. Abdi, M. Aillerie, P. Bourson, and M. D. Fontana, *J. Appl. Phys.* 84, 2251 **(1998)**.
4. P. Sen, P. K. Sen, R. Bhatt, S. Kar, V. Shukla, and K. S. Bartwal, *Solid State Commun.* 129, 747 **(2004)**.
5. M. Niederberger, N. Pinna, J. Polleux, and M. Antonietti, *Angew. Chem. Int. Ed.* 43, 2270 **(2004)**.
6. K. Niwa, Y. Furukawa, S. Takakawa, and K. Kitamura, *J. Cryst. Growth* 208, 493 **(2000)**.
7. M. Liu and D. Xue, *Solid State Ionics* 177, 275 **(2006)**.
8. V. T. Kalinnikov, O. G. Gromov, G. B. Kunshina, A. P. Kuz'min, E. P. Lokshin, and V. I. Ivanenko, *Inorg. Mater.* 40, 411 **(2004)**.
9. S. C. Navale, V. Samuel, and V. Ravi, *Ceram. Int.* 32, 847 **(2006)**.
10. S. D. Chang, C. H. Kam, Y. Z. Zhou, Y. L. Lam, Y. C. Chan, and S. Buddhudu, *Mat. Lett.* 45, 19 **(2000)**.
11. C. An, K. Tang, C. Wang, G. Shen, Y. Jin, and Y. Qian, *Mater. Res. Bull.* 37, 1791 **(2002)**.
12. C. Luo and D. Xue, *Langmuir* 22, 9914 **(2006)**.
13. P. Afanasiev, *Mat. Lett.* 34, 253 **(1998)**.
14. E. R. Camargo and M. Karkihana, *Solid State Ionics* 151, 413 **(2002)**.
15. M. Aufray, S. Menuel, Y. Fort, J. Eschbach, D. Rouxel, and B. Vincent, *J. Nanosci. Nanotechnol.* 9, 4780 **(2009)**.
16. B. L. Cushing, V. L. Kolesnichenko, and C. J. O'Connor, *Chem. Rev.* 104, 3893 **(2004)**.

17. R. Dwivedi, A. Maurya, A. Verma, R. Prasad, and K. S. Bartwal, *J. Alloys Compd.* 509, 6848 **(2011)**.
18. N. Kaithwas, M. Dave, S. Kar, and K. S. Bartwal, *Physica E* 44, 1486 **(2012)**.
19. A. Majchrowski, J. Ebothe, E. Gondek, K. Ozga, I. V. Kityk, A. H. Reshak, and T. Łukasiewicz, *J. Alloys Compd.* 485, 29 **(2009)**.
20. Y. Djaoued, K. Ozga, A. Wojciechowski, A. H. Reshak, J. Robichaud, and I. V. Kityk, *J. Alloys Compd.* 508, 599 **(2010)**.
21. A. Hussain, A. P. Jadhav, Y. K. Baek, H. J. Choi, J. Lee, and Y. S. Kang, *J. Nanosci. Nanotechnol.* 13, 7717 **(2013)**.
22. E. R. Leite, Encyclopedia of Nanoscience and Nanotechnology, edited by H. S. Nalwa, American Scientific Publishers, LA **(2004)**, Vol. 6, p. 537.
23. M. M. Barbooti and D. A. Al-Sammerrai, *Thermochim Acta* 98, 119 **(1986)**.
24. G. Pezzotti, H. Hagihara, and W. Zhu, *J. Phys. D: Appl. Phys.* 46, 145103 **(2013)**.
25. I. P. Kaminow and W. D. Johnston, *Phys. Rev.* 160, 519 **(1967)**.
26. U. Schlarb, S. Klauer, M. Wesselmann, K. Betzler, and M. Wöhlecke, *Appl. Phys. A* 56, 311 **(1993)**.
27. A. Ridah, P. Bourson, M. D. Fontana, and G. Malovichko, *J. Phys.: Condens. Matter* 9, 9687 **(1997)**.
28. A. Bartasyte, V. Plausinaitiene, A. Abrutis, S. Stanionyte, S. Margueron, P. Boulet, T. Kobata, Y. Uesu, and J. Gleize, *J. Phys.: Condens. Matter.* 25, 205901 **(2013)**.

Received: 4 December 2013. Accepted: 21 March 2014.